Effect of backleak in nephron dynamics

P. G. Kevrekidis and N. Whitaker
Department of Mathematics and Statistics, University of Massachusetts, Amherst, Massachusetts 01003-4515, USA
(Received 18 December 2002; published 23 June 2003)

The effect of transepithelial solute, i.e., sodium chloride, backleak is taken into consideration in the spatiotemporal evolution of the chloride concentration along the thick ascending limb of a single nephron. The importance of the mechanism and of its mathematical modeling is argued on physiological grounds. The backleak ''strength'' is found to significantly modify the threshold for the appearance of temporally oscillatory behavior in the chloride concentration in the thick ascending limb which has previously been experimentally observed in normotensive rats.

DOI: 10.1103/PhysRevE.67.061911 PACS number(s): 87.10.+e

In the past few years, there has been an increasing number of studies of nephron dynamics. The nephron is the functional unit of the kidney; the human kidney consists of $\approx 10^6$ such units [1]. Naturally, in light of this large number, one can take different paths in studying the dynamics of physiological processes in the kidney.

One approach focuses on a single nephron and the functions that it performs [2–4]. In this setting [2–4], one examines the flow of blood through the filtering processes of the nephron. Blood enters through the afferent arteriole into the glomerulus, where its constituents are filtered and large molecular weight contents, such as blood cells and proteins, are retained. On the contrary, low molecular weight substances proceed through the proximal tubule to the loop of Henle. The membranes which separate the tubules from the interstitium are permeable to certain substances causing further filtering. The interstitium is the region around the nephron consisting of fine, reticular fibrils. The low molecular weight substances move between the limbs of the loop of Henle and the interstitium through active and passive (backleak or diffusion) processes. These substances then proceed from the thick ascending limb of the loop to the distal tubule where the macula densa cells exert a negative delayed feedback to the incoming blood flow. This is the so-called tubuloglomerular feedback or TGF. The macula densa ''measure'' the concentration levels of the NaCl flowing through the upper part of the distal tubule (before the collecting duct where the resulting filtrates are collected) and accordingly decide to constrict the afferent arteriole, if the NaCl concentration is high, or not. The TGF mechanism is very important for the stabilization of the renal blood flow in response to arterial blood pressure fluctuations. A schematic diagram of the above process is presented in Fig. 1 which is very similar to Fig. 3 in Ref. [5].

It has been observed experimentally that the TGF system can exhibit temporal limit cycle oscillations in certain variables, including the fluid flow, the pressure, and the tubular fluid NaCl concentration in the early distal tubule, see, e.g., Refs. [6–8]. These are nonsinusoidal, nonlinear temporal oscillations [9,10], with periods of the order of tens of seconds [5] which occur due to the delicate interplay between transport and feedback mechanisms [2,11]. In Ref. [2–4], these limit cycle oscillations were observed numerically. However, the analysis was introduced but did not examine in detail the effects of backleak (simple diffusion).

In this work, we focus on the study of solute transport through the thick ascending limb of a single nephron continuing along the line of study originally proposed by Refs. [2–4]. The main contribution of this paper is the detailed study of an important factor, namely, the transepithelial solute, i.e., chloride, backleak from the interstitium back to the thick ascending limb of the loop of Henle. This contribution was introduced, but was subsequently neglected in the analysis of Ref. [2]. The aims of the present work are (1) to physiologically motivate the inclusion of the backleak; (2) to present the analysis for incorporating such a term along the vein introduced in Ref. [2]; (3) to examine the phenomenology of the single-nephron dynamics in the presence of the backleak and to compare it with the case in which the backleak is absent.

The manifestation of the analytical tractability and the analytical and numerical evidence for the importance of including such a mechanism are the distinguishing features of the present work with respect to previous ones. In particular, this study constitutes a fuller analysis of the model constructed in Ref. [2].

Our presentation proceeds as follows: we first present the mathematical model and explain the relevance of the inclu-

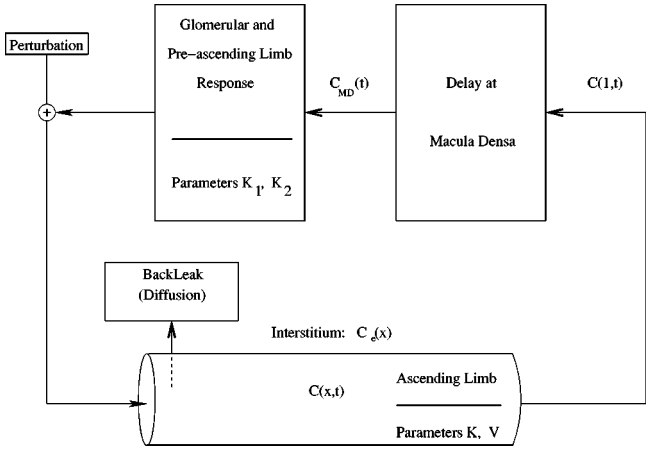

FIG. 1. A schematic representation of the nephron adapted from Ref. [5].

sion of the backleak diffusion mechanism. We demonstrate the ways in which the backleak term can be incorporated into the theory and examine the relevant results analytically as well as numerically. We then summarize our findings and conclude.

In the spirit of Refs. [2,4], we will consider the following transport model for the chloride concentration along the thick ascending limb of the loop of Henle:

$$C_t(x,t) = -F(C(1,t-\tau))C_x(x,t) - \frac{VC(x,t)}{K+C(x,t)} - P(C(x,t)-C_{ext}(x)), \quad (1)$$

where

$$F(x) = 1 + K_1 \tanh[K_2(C_{op}-x)].$$

Equation (1) assumes that the nephron is treated as diffusion in a rigid tube of unit length ($x=1$), and all quantities are dimensionless according to the rescaling of Ref. [2]. The model is based on the mass conservation of chloride, classifying its transport as occurring due to three key processes.

(1) The TGF induced axial chloride advection at intratubular flow speed F. This mechanism incurs the time delay τ. K_1 and K_2 are constants and C_{op} is the concentration of the steady solution $S(x)$ at the end of the thick ascending limb of the loop of Henle. The steady state $S(x)$ occurs for $F=1$.

(2) The efflux of the solute into the interstitium due to active processes, i.e., metabolic pumps in the tubular walls. This is assumed to be occurring by means of the Michaelis-Menten kinetics with maximum transport rate V and Michaelis constant K.

(3) Finally, and most importantly for this presentation, the transepithelial chloride backleak which depends on the fixed interstitial chloride concentration profile C_{ext} and its gradient with respect to the tubular profile. This last term is proportional to the chloride permeability P.

We briefly analyze initially the case without the backleak, i.e., $P=0$. Then, the steady state problem can be solved, in the implicit form

$$-Vx = K\ln\left(\frac{C}{C_0}\right) + C - C_0, \quad (2)$$

where C_0 is the concentration at the starting point of the thick ascending limb, i.e., $x=0$.

Analytically, tractable simplifications of Eq. (2) can be given in two different settings.

(1) For very small NaCl transport rates (e.g., for maximum transport rate $V \ll 1$), in which case the concentration can be approximated to second order as

$$C = C_0 + C_0(a_1 - \sqrt{a_1^2 + b_1 x}), \quad (3)$$

where $a_1=(C_0+K)/K$ and $b_1=2V/K$. Notice that the leading order approximation for the spatial decrease in concentration is linear.

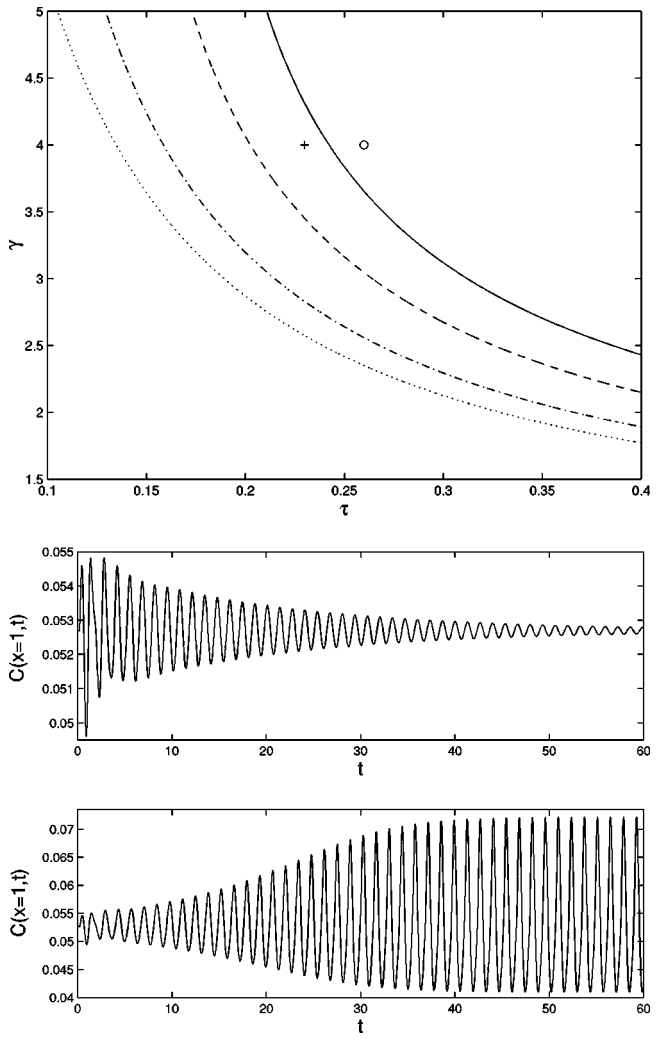

FIG. 2. The locus of points of the Hopf bifurcation in the γ-τ plane is shown in the top panel. Below the curves, the steady state solution is stable, while above the curves the Hopf bifurcation sets in. The dotted line corresponds to $R=0$, the dash-dotted to $R=0.1$, the dashed to $R=0.3$, and the solid to $R=0.5$. The plus and circle, correspond, respectively, to the cases whose numerical time evolution (at the end point of the thick ascending limb $x=1$) is shown in the bottom panel of the figure. The plus corresponds to the $(\gamma,\tau)=(4,0.23)$ which is stable for $R=0.5$, while the circle to $(\gamma,\tau)=(4,0.26)$ which is unstable, as confirmed by the dynamical evolution.

(2) For $K \gg C_0 > C$, i.e., for very weak, practically linear in C, active transport, in which case to second order the steady state, spatial concentration decay can be approximated by

$$C = \frac{a_2}{b_2 + G\exp(a_2 x)}, \quad (4)$$

where $G=(a_2-b_2C_0)/C_0$, $a_2=V/K$ and $b_2=V/K^2$. To leading order, here the decay is exponential.

The main theme of earlier studies was to examine the stability of the above steady state [2–4]. In particular, experimental evidence for rats indicated that both steady state and limit cycle temporal behavior of the solute concentration at the end point of the thick ascending limb were possible. These types of behavior occur under physiological conditions for different values of the feedback delay, and of the TGF advection rate. The backleak mechanism was included in the model but was subsequently neglected, predominantly due to its mathematical intractability. However, in this paper, we reexamine this topic and make a case for the inclusion of the latter factor due to the following:

(1) In many cases, the administering of diuretics, and in particular osmotic diuretics such as mannitol, allows increased passive backleak of solutes through the paracellular pathway [12]. This indicates that the incorporation of the last term of Eq. (1) is particularly relevant in modeling such processes.

(2) In the case of acute renal failures, the backleak of the glomerular filtrate through abnormally permeable tubular epithelia occurs [13]. Hence to model such abnormalities, it is important to include backleak terms.

Even though in this study we do not address specific cases of renal failures and pharmacological treatments thereof, we examine *quantitatively* the effects of the backleak.

We first consider the general case of solute backleak inclusion, in fact, for a more general setting than Eq. (1), i.e., for general solute transport kinetics $J(C)$, namely, for a steady equation of the form

$$C_x = -J(C) - P(C - C_{ext}). \tag{5}$$

Following Ref. [2], we call the solution of Eq. (5) $S(x)$ and examine the stability of the linearization around such a solution using the expansion $C(x,t) = S(x) + \epsilon D(x,t)$, where ϵ is the formal linearization parameter and substitution of the linearization ansatz into the dynamical transport equation yields to $O(\epsilon)$,

$$D_t = -D_x - J'(C)D + rS'(x)D(1,t-\tau) - PD, \tag{6}$$

where $r = -F'(S(x))$. The prime will be used to denote derivative with respect to the functional argument. As is typical in linearization expansions, we separate the temporal from the spatial dependence of $D(x,t)$ according to $D(x,t) = f(x)\exp(\lambda t)$. Then the eigenvalues λ of the linearization contain the information about the stability of the steady state. If $\mathrm{Re}(\lambda) < 0$, then the steady state is dynamically stable, while the zero crossing (going from negative to positive) of the real part of the eigenvalue will signal the transition to instability and to oscillatory behavior due to this so-called Hopf bifurcation. Using the above separation of variables, Eq. (6) is transformed into an ordinary differential equation (ODE) for f which is linear and can be solved as

$$f(x) = rf(1)\exp[-\lambda\tau - h(x)] \int_0^x S'(y)\exp[h(y)]dy, \tag{7}$$

with $h(x) = \lambda x - \ln[S'(x)/S'(0)] + P\int_0^x [C'_{ext}/S'(u)]du$. However, in this particular problem, due to the presence of the delay, a compatibility condition needs to be enforced at $x = 1$, providing an explicit equation for the eigenvalue in the form

$$\exp[\lambda(1+\tau)] = -\gamma \int_0^1 dy \exp\left(\lambda y + P \int_1^y \frac{C'_{ext}}{S'(u)} du \right), \tag{8}$$

where $\gamma = -rS'(1)$. We will examine two particular cases of Eq. (8).

(1) The simplest and most physiologically realistic one is the case where $C_{ext} = qS(x) + q_1$, where q, q_1 are constants. This case which, in our view, appears to be the simplest one in terms of mathematical tractability, also appears to be very interesting from a physiological point of view. In particular, the schematic of p. 106 of Ref. [1] showing the interstitial solute concentration for corresponding profiles of the thick ascending limb concentration clearly indicates that the above prescription of C_{ext} is physiologically relevant at steady state. In this case, the equation for the eigenvalue becomes

$$1 = \gamma \exp(-\lambda\tau) \frac{\exp(-\lambda - Pq) - 1}{\lambda + Pq}. \tag{9}$$

This is a straightforward generalization of the eigenvalue condition of Refs. [2–4], which reduces to the latter one for $P = 0$. Notice that in this case the profile S is given by the quadrature $x = \int_{C_0}^{S} dC(K+C)/[AC^2 + (B - V + AK)C + BK]$, with $A = P(1-q)$ and $B = Pq_1K$. In the case of Eq. (9), as mentioned above, the instability occurs when the (in general complex) eigenvalue $\lambda = \zeta + i\omega$ crosses the imaginary axis, i.e., when $\zeta = 0$. Hence the instability criterion can be written as

$$[e^{-Pq}\cos(\omega) - 1][\omega\cos(\omega\tau) + Pq\sin(\omega\tau)] + e^{-Pq}\sin(\omega) \times [Pq\cos(\omega\tau) - \omega\sin(\omega\tau)] = 0, \tag{10}$$

$$\gamma = \frac{(Pq)^2 + \omega^2}{[e^{-Pq}\cos(\omega) - 1][-\omega\sin(\omega\tau) + Pq\cos(\omega\tau)] - e^{-Pq}\sin(\omega)[Pq\sin(\omega\tau) + \omega\cos(\omega\tau)]}. \tag{11}$$

(2) Alternative cases that can be examined are the ones of Eqs. (3) and (4). However, the former is quite complicated due to the polynomial nature of the dependence. In the latter case, upon the simplifying assumption of $C=C_0\exp(-a_2x)$, we can find the corresponding profile of $C_{ext}\approx C_0\exp(-ax)-(VC_0^2/PK^2)\exp(-2a_2x)$. Notice that here we use Eq. (1) as an inverse problem: we postulate C, and find the corresponding C_{ext}; we do that approximately here for simplicity. Then the corresponding eigenvalue condition can be obtained as

$$1=\gamma\exp(-\lambda\tau)\frac{\exp[-\lambda-P(1-Q)]-1}{\lambda+P(1-Q)}, \qquad (12)$$

where $Q=2VC_0/(PK^2)$ and $V/K\ll 1$ has been used. Once again, one can find the instability threshold conditions of Eqs. (10)–(11), which we omit for the sake of brevity.

We now turn to numerical results. In particular, we examine the locus of points of the Hopf bifurcation in the γ-τ plane, for various values of the permeability P, to determine how the backleak affects the onset of the oscillatory behavior. We study this effect in the most physiologically realistic case among the ones mentioned above, namely, the case where the external solute concentration is proportional to the steady state one [1]. Equations (10) and (11) determine for a given TGF delay time, and the backleak strength $R=Pq$, the oscillation frequency ω, as well as γ which is related to the advection rate, exactly at the critical case, i.e., at the onset of the oscillatory behavior. These curves are shown in the top panel of Fig. 2 in the γ-τ plane, similarly as in Refs. [2–4], but for different values of R. When $R=0$, we retrieve the original case of Refs. [2–4]. However, and this is one of the main findings of this work, these curves can be *significantly shifted* by the consideration of a very relevant physiological mechanism such as the inclusion of the backleak.

To further illustrate that point we note that below the shown curves, the steady state solution will be stable for a given R, while above them the Hopf bifurcation will lead to a time-periodic behavior. We thus choose two cases both of which would be unstable for $R=0$ (i.e., without backleak), but one of which is unstable (circle) while the other is stable (star) for $R=0.5$. The corresponding results of dynamical time evolution of the two cases for $R=0.5$ are shown in the bottom panel of Fig. 2, clearly confirming the theoretical prediction and highlighting how *the inclusion of the backleak may have a stabilizing effect in the spatiotemporal evolution of solute concentration in a single nephron.*

In this paper, we have examined systematically the effects of the inclusion of the solute backleak in the dynamical evolution and stability of NaCl concentration profiles over a single nephron of the kidney. We have found that this factor, which is important, as we have argued, in a number of settings, may significantly modify the predicted threshold for the oscillatory behavior observed in experiments [14,15].

[1] A.J. Vander, *Renal Physiology*, 5th ed. (McGraw-Hill, New York, 1995).

[2] H.E. Layton, E.B. Pitman, and L.C. Moore, Am. J. Physiol. Renal Physiol. **261**, F904 (1991).

[3] R. M. Zaritski, Ph.D. thesis, State University of New York, Buffalo, NY, 1999.

[4] B.E. Pitman, R.M. Zaritski, L.C. Moore, and H.E. Layton, in *The IMA Volumes in Mathematics and its Applications*, edited by H.E. Layton and A.M. Weinstein (Springer-Verlag New York, 2002), Vol. 129, p. 345.

[5] H.E. Layton, E.B. Pitman, and L.C. Moore, Am. J. Physiol. Renal Physiol. **278**, F287 (2000).

[6] N.-H. Holstein-Rathlou and D.J. Marsh, Am. J. Physiol. **256**, F1007 (1989).

[7] P.P. Leyssac and L. Baumbach, Acta Physiol. Scand. **117**, 415 (1983).

[8] P.P. Leyssac, F.M. Karlsen, and O. Skott, Am. J. Physiol. Renal Physiol. **261**, F169 (1991).

[9] K.-P. Yip, N.-H. Holstein-Rathlou, and D.J. Marsh, Am. J. Physiol. Renal Physiol. **261**, F400 (1991).

[10] K.-P. Yip, N.-H. Holstein-Rathlou, and D.J. Marsh, Am. J. Physiol. Renal Physiol. **264**, F427 (1993).

[11] N.-H. Holstein-Rathlou and D.J. Marsh, Am. J. Physiol. Renal Physiol. **258**, F1448 (1990).

[12] See, e.g., Sec. XIV of hsc.virginia.edu/med-ed/phys/pdf/ecfreg.pdf

[13] H.F. Galley, J. R. Coll. Surg. Edinb **45**, 44 (2000).

[14] N.-H. Holstein-Rathlou and D.J. Marsh, Am. J. Physiol. **256**, F1007 (1989).

[15] N.-H. Holstein-Rathlou and D.J. Marsh, Physiol. Rev. **74**, 637 (1994).